(pAIM65). The luciferase expressing, wild-type Gam1 (CELOwt) and the CELO virus purification on CsCl gradients have been described (CELO AIM46; ref. 24). The CELOdGhsp40 and CELOdGhsp70 genomes were constructed by exchanging the CMV/luciferase/β-globin cassette for CMV/hsp40/β-globin or CMV/hsp70/β-globin cassettes.

Analysis of the replication of CELOdG (Fig. 5a) was performed by transfecting the CELOdG genome into LMH cells alone, or followed by infection with 1,000 particles per cell of AdGam1 after 24 h. After 5 days, we collected the cells and assayed them for luciferase activity. We used an additional culture to infect a fresh set of LMH cultures either alone, or with AdGam1. We repeated the cell collection, luciferase assay and passage every 5 days for 5 passages.

Immunoblotting analysis

We lysed A549 cells in lysis buffer (150 mM NaCl, 50 mM Tris, pH 7.5, 5 mM EDTA, 1% NP-40 containing protease inhibitor cocktail; Sigma). Cells were agitated at 4 °C for 30 min, passaged through a 25 gauge needle 5 times, sonicated in a bath sonicator for 5 min, and centrifuged at 14,000 r.p.m. (Eppendorf) for 5 min, and the supernatant was used for immunoblotting analysis. Equal quantities of protein (measured by Bradford reagent, Pierce) were resolved by polyacrylamide gel electrophoresis (PAGE), transferred to nitrocellulose and probed with the indicated antiserum preparations (see below). Antibody binding was revealed using the appropriate peroxidase-conjugated secondary antibodies (Dako) and ECL reagents (Amersham).

Immunofluorescence

Cells were plated on glass cover slips (12 × 12 mm) in 6-well dishes 24 h before transfection or infection. Cells were fixed one day after transfection/infection in 4% paraformaldehyde for 15 min, rinsed 3 times with PBS, permeabilized with PBS/0.1% Triton X-100 (PBT) for 15 min, blocked in 5% BSA/PBT for 30–60 min, incubated with primary antibody for 15 min in 5% BSA/PBT, washed 3 times with PBT, incubated with secondary antibody for 15 min in 5% BSA/PBT, washed 2 times with PBT, washed 2 times with PBS, and mounted in 50% glycerol/PBS, 10 mM Tris pH 8.5, 4% *n*-propyl gallate (Sigma); all incubations were done at room temperature. DNA was stained with Hoechst dye. Images were acquired with a cooled CCD camera (Spot II; Diagnostic Instruments) mounted on an Axiovert microscope (Zeiss) equipped with 63×/1.4 lens with filters from Chroma Tech and processed using Adobe Photoshop software.

We used the following antiserum preparations: murine monoclonal 9E10 recognizing the Myc epitope[28]; murine monoclonal RPN-1197 recognizing hsp70 (Amersham) or goat polyclonal sera recognizing hsp70, hsp40, hsp90α, hsc70 and hsp27 (Santa Cruz Biotechnology); anti-tubulin (clone DM1A, Sigma); and a rabbit polyclonal directed against total capsid proteins[24]. We used the following secondary antibodies: DTAF conjugated donkey anti mouse, DTAF conjugated donkey anti rabbit and Cy3 conjugated donkey anti goat (Jackson Laboratories).

We carried out transfections using a double PEI technique as described[24]. LMH cells[29] and A549 cells (ATCC CCL-185) were cultured in DMEM plus 10% FCS (DMEM, 2 mM glutamine, 100 IU penicillin, 100 μg ml^{-1} streptomycin and 10% (v/v) fetal calf serum). The 293 cell line[30] was cultured in MEMalpha with 10% newborn calf serum.

Received 24 January; accepted 23 June 2000.

1. Nevins, J. R. Induction of the synthesis of a 70,000 dalton mammalian heat shock protein by the adenovirus E1A gene product. *Cell* **29,** 913–919 (1982).
2. Kao, H. T. & Nevins, J. R. Transcriptional activation and subsequent control of the human heat shock gene during adenovirus infection. *Mol. Cell. Biol.* **3,** 2058–2065 (1983).
3. Phillips, B., Abravaya, K. & Morimoto, R. I. Analysis of the specificity and mechanism of transcriptional activation of the human hsp70 gene during infection by DNA viruses. *J. Virol.* **65,** 5680–5692 (1991).
4. Santomenna, L. D. & Colberg-Poley, A. M. Induction of cellular hsp70 expression by human cytomegalovirus. *J. Virol.* **64,** 2033–2040 (1990).
5. Ohgitani, E., Kobayashi, K., Takeshita, K. & Imanishi, J. Biphasic translocation of a 70 kDa heat shock protein in human cytomegalovirus-infected cells. *J. Gen. Virol.* **80,** 63–68 (1999).
6. Kobayashi, K. *et al.* Herpes simplex virus-induced expression of 70 kDa heat shock protein (HSP70) requires early protein synthesis but not viral DNA replication. *Microbiol. Immunol.* **38,** 321–325 (1994).
7. Collins, P. L. & Hightower, L. E. Newcastle disease virus stimulates the cellular accumulation of stress (heat shock) mRNAs and proteins. *J. Virol.* **44,** 703–707 (1982).
8. Mayer, M. P. & Bukau, B. HSP70 chaperone systems: diversity of cellular functions and mechanism of action. *Biol. Chem.* **379,** 261–268 (1998).
9. Kelley, W. L. Molecular chaperones: How J domains turn on Hsp70s. *Curr. Biol.* **9,** R305–308 (1999).
10. Flint, J. & Shenk, T. Viral transactivating proteins. *Annu. Rev. Genet.* **31,** 177–212 (1997).
11. Chiocca, S., Baker, A. & Cotten, M. Identification of a novel anti-apoptotic protein, GAM-1, encoded by the CELO adenovirus. *J. Virol.* **71,** 3168–3177 (1997).
12. Gabai, V. L. *et al.* Hsp70 prevents activation of stress kinases. A novel pathway of cellular thermotolerance. *J. Biol. Chem.* **272,** 18033–18037 (1997).
13. Mosser, D. D. *et al.* Role of the human heat shock protein hsp70 in protection against stress-induced apoptosis. *Mol. Cell. Biol.* **17,** 5317–5327 (1997).
14. Welch, W. J. & Feramisco, J. R. Nuclear and nucleolar localization of the 72,000-dalton heat shock protein in heat-shocked mammalian cells. *J. Biol. Chem.* **259,** 4501–4513 (1984)
15. Hattori, H. *et al.* Intracellular localization and partial amino acid sequence of a stress-inducible 40-kDa protein in HeLa cells. *Cell. Struct. Funct.* **17,** 77–86 (1992).
16. Polissi, A., Goffin, L. & Georgopoulos, C. The *Escherichia coli* heat shock response and bacteriophage lambda development. *FEMS Microbiol. Rev.* **17,** 159–169 (1995).
17. Liu, J. S. *et al.* Human Hsp70 and Hsp40 chaperone proteins facilitate human papillomavirus-11 E1 protein binding to the origin and stimulate cell-free DNA replication. *J. Biol. Chem.* **273,** 30704–30712 (1998).
18. Campbell, K. S. *et al.* DnaJ/hsp40 chaperone domain of SV40 large T antigen promotes efficient viral DNA replication. *Genes Dev.* **11,** 1098–1110 (1997).
19. Kelley, W. L. & Georgopoulos, C. The T/t common exon of simian virus 40, JC, and BK polyomavirus T antigens can functionally replace the J-domain of the *Escherichia coli* DnaJ molecular chaperone. *Proc. Natl Acad. Sci. USA* **94,** 3679–3684 (1997).
20. Stubdal, H. *et al.* Inactivation of pRB-related proteins p130 and p107 mediated by the J domain of simian virus 40 large T antigen. *Mol. Cell. Biol.* **17,** 4979–4990 (1997).
21. Srinivasan, A. *et al.* The amino-terminal transforming region of simian virus 40 large T and small t antigens functions as a J domain. *Mol. Cell. Biol.* **17,** 4761–4773 (1997).
22. Chiocca, S. *et al.* The complete DNA sequence and genomic organization of the avian adenovirus CELO. *J. Virol.* **70,** 2939–2949 (1996).
23. Chartier, C. *et al.* Efficient generation of recombinant adenovirus vectors by homologous recombination in *Escherichia coli*. *J. Virol.* **70,** 4805–4810 (1996).
24. Michou, A. -I., Lehrmann, H., Saltik, M. & Cotten, M. Mutational analysis of the avian adenovirus CELO, which provides a basis for gene delivery vectors. *J. Virol.* **73,** 1399–1410 (1999).
25. Ohtsuka, K. Cloning of a cDNA for heat-shock protein hsp40, a human homologue of bacterial DnaJ. *Biochem. Biophys. Res. Commun.* **197,** 235–240 (1993).
26. Hunt, C. & Morimoto, R. I. Conserved features of eukaryotic hsp70 genes revealed by comparison with the nucleotide sequence of human hsp70. *Proc. Natl Acad. Sci. USA* **82,** 6455–6459 (1985).
27. Stratford-Perricaudet, L. D., Makeh, I., Perricaudet, M. & Briand, P. Widespread long-term gene transfer to mouse skeletal muscles and heart. *J. Clin. Invest.* **90,** 626–630 (1992).
28. Evan, G. I., Lewis, G. K., Ramsay, G. & Bishop, J. M. Isolation of monoclonal antibodies specific for human c-myc proto-oncogene product. *Mol. Cell. Biol.* **5,** 3610–3616 (1985).
29. Kawaguchi T., Nomura, K., Hirayama, Y. & Kitagawa, T. Establishment and characterization of a chicken hepatocellular carcinoma cell line, LMH. *Cancer Res.* **47,** 4460–4464 (1987).
30. Graham F. L., Smiley, J., Russell, W. C. & Nairn, R. Characteristics of a human cell line transformed by DNA from human adenovirus type 5. *J. Gen. Virol.* **36,** 59–74 (1977).

Acknowledgements

We thank M. Raff for suggesting the heat-shock complementation and G. Christofori for his comments on the manuscript. We thank K. Ohtsuka for the hsp40 cDNA and S. Fox and R. Morimoto for the hsp70 gene.

Correspondence and requests for materials should be addressed to M.C. (e-mail: cotten@nt.imp.univie.ac.at).

Peroxynitrite reductase activity of bacterial peroxiredoxins

Ruslana Bryk*, Patrick Griffin† & Carl Nathan*

** Department of Microbiology and Immunology, Weill Medical College of Cornell University, New York, New York 10021, USA*
† Basic Chemistry Analytical Support, Merck Research Laboratories, Rahway, New Jersey 07065, USA

Nitric oxide (NO) is present in soil and air, and is produced by bacteria, animals and plants. Superoxide (O_2^-) arises in all organisms inhabiting aerobic environments. Thus, many organisms are likely to encounter peroxynitrite ($OONO^-$), a product of NO and O_2^- that forms at near diffusion-limited rates, and rapidly decomposes upon protonation through isomerization to nitrate (NO_3^-; ref. 1) while generating hydroxyl radical ($^{\bullet}OH$) and nitrogen dioxide radical ($^{\bullet}NO_2$) (refs 2, 3), both more reactive than peroxynitrite's precursors. The oxidative, inflammatory, mutagenic and cytotoxic potential (ref. 4) of peroxynitrite contrasts with the antioxidant, anti-inflammatory and tissue-protective properties ascribed to NO itself[5]. Thus, the ability of cells to cope with peroxynitrite is central in determining the biological consequences of NO production. We considered whether cells might be equipped with enzymes to detoxify peroxynitrite. Peroxiredoxins have been identified in most genomes sequenced, but their functions are only partly understood. Here we show that the peroxiredoxin alkylhydroperoxide reductase subunit C (AhpC) from *Salmonella typhimurium* catalytically detoxifies peroxynitrite to nitrite fast enough to forestall the oxidation of bystander molecules such as DNA. Results are similar with peroxiredoxins from *Mycobacterium tuberculosis* and *Helicobacter pylori*. Thus,

peroxynitrite reductase activity may be widespread among bacterial genera.

Enzymatic activities have been demonstrated for only a few of the proteins encoded by several hundred peroxiredoxin sequences, namely, the reduction of alkyl or hydrogen peroxides to alcohols or water[6]. The first peroxiredoxin purified, AhpC, was identified in *Escherichia coli* and *S. typhimurium* along with its flavoprotein partner AhpF as products of a bicistronic operon within the H_2O_2-activatable oxyR regulon[7]. We recently demonstrated that an *ahpCF*-deficient mutant of *S. typhimurium* was markedly sensitized to bactericidal effects of nitrite and *S*-nitrosoglutathione[8]. Resistance was restored by transformation with *ahpC* from *S. typhimurium* or *M. tuberculosis*. Moreover, transfection with *ahpC* from *M. tuberculosis* protected human cells from death caused by nitric oxide synthase-2 (NOS2)[8]. Host defence against experimental tuberculosis depends on production of reactive nitrogen intermediates by NOS2[9], and antisense-mediated decrease in expression of *ahpC* abolished the virulence of *Mycobacterium bovis*[10]. Thus, peroxiredoxins can protect cells from reactive nitrogen intermediates, and we hypothesized that peroxiredoxins do so by acting as peroxynitrite reductases.

We tested this hypothesis using pure *S. typhimurium* AhpC, reagent peroxynitrite, and target molecules susceptible to oxidation.

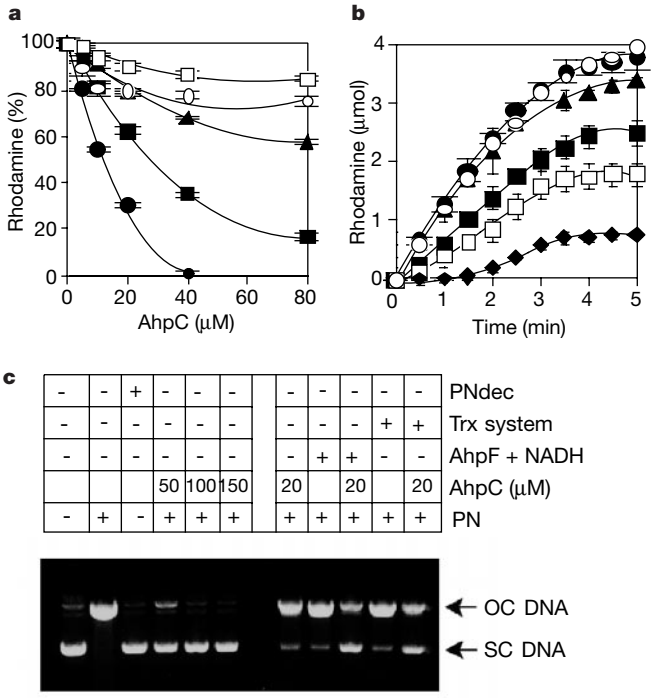

Figure 1 AhpC from *S. typhimurium* protects dihydrorhodamine and DNA from peroxynitrite-induced oxidation. **a**, Protection of dihydrorhodamine without catalytic turnover of AhpC. Reactions contained KPi buffer with 100 μM dihydrorhodamine and indicated concentrations of AhpC, either wild-type (filled circles), mutant C165A (filled squares), C46A (filled triangles), or C46/165A (open circles), or AhpC pre-oxidized with TBH (open squares). Peroxynitrite (20 μM) was added and rhodamine formation measured by absorbance at 500 nm wavelength. **b**, Protection of dihydrorhodamine during catalytic turnover of AhpC. Reactions as in **a** also contained 50 μM NADH and no protein (filled circles), 1 μM AhpC alone (open circles), 5 μM AhpF alone (filled triangles), or 5 μM AhpF plus AhpC at 1 μM (filled squares), 5 μM (open squares) or 10 μM (diamonds). Peroxynitrite was infused to achieve 8.4 μM min^{-1} for 5 min. **c**, Protection of DNA. Reactions contained 1 μg of pBluescript II plasmid and indicated amounts of AhpC with or without 500 nM AhpF and 50 μM NADH, or 0.5 units of TR, 2 μM Trx and 50 μM NADPH (Trx system) in KPi buffer pH 6.5. Peroxynitrite (PN) or decomposed peroxynitrite (PNdec) was infused to achieve 25 μM min^{-1} for 3 min. Agarose gel electrophoresis separated supercoiled (SC) and open circular (nicked) (OC) DNA. All results are from ≥3 experiments (error bars show ± s.d.).

At a molar excess of AhpC over peroxynitrite, AhpC protected dihydrorhodamine completely against oxidation (Fig. 1a). Mutation of Cys 165 to Ala (C165A) diminished the protective effect of AhpC slightly. The mutant C46A was markedly less effective than wild type, and the double mutant C46/165A was scarcely protective. Likewise, protection was lost when the Cys residues in AhpC were oxidized by pre-exposure to *t*-butyl hydroperoxide (TBH) (Fig. 1a). Next we tested whether AhpC could act catalytically during perfusion with peroxynitrite in molar excess (Fig. 1b). Under these conditions, AhpC alone did not protect dihydrorhodamine unless we also provided pure AhpF and NADH to reduce AhpC. With the full system, AhpC displayed a concentration-dependent ability to protect dihydrorhodamine from a 40-fold molecular excess of peroxynitrite during 5 min of perfusion (Fig. 1b). DNA is a critical physiological target of peroxynitrite[11]. At a molar excess of AhpC over peroxynitrite, AhpC alone protected supercoiled DNA from

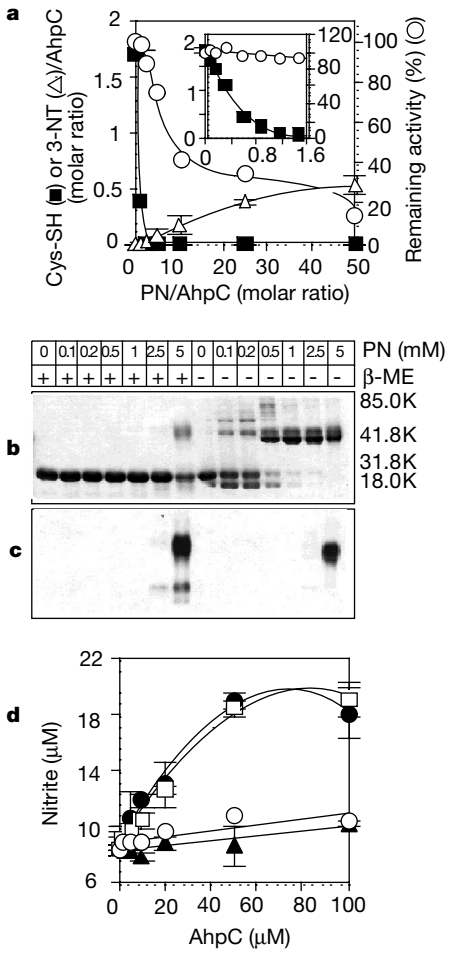

Figure 2 Catabolism of peroxynitrite by AhpC. **a**, Reversible oxidation of Cys residues. Samples of AhpC (100 μM) were pretreated with excess peroxynitrite (PN) as indicated, then assayed for TBH reductase activity (open circles), free Cys-SH content (filled squares), and 3-nitrotyrosine (3-NT) (open triangles). Inset, results at a low excess of peroxynitrite. **b**, Intermonomeric disulphide bond formation and cross-linking. AhpC treated with excess peroxynitrite as in **a** was boiled for 5 min in Laemmli buffer with or without β-mercapthoethanol (β-ME), separated by SDS–polyacrylamide gel electrophoresis and stained with Coomassie. Numbers on right, relative molecular mass M_r. **c**, Western blot with anti-nitrotyrosine monoclonal antibody (1 μg, Alexis) using a duplicate of the gel shown in **b**. **d**, Nitrite formation: dependence on Cys 46. Peroxynitrite (20 μM) was added to 100 μl of KPi buffer in the presence of indicated amounts of AhpC, either wild-type (filled circles) or mutants C46A (filled triangles), C165A (open squares) or C46/165A (open circles) for 15 min before measuring nitrite. All results are from ≥3 experiments (error bars show ± s.d.).

single-strand breaks. At a molar excess of peroxynitrite over AhpC, protection was evident only in the presence of AhpC + AhpF + NADH, or AhpC + thioredoxin reductase (TR) + thioredoxin (Trx) + NADPH (Fig. 1c).

To test if peroxynitrite reversibly oxidizes the Cys residues of AhpC, we pretreated AhpC with peroxynitrite at a 0.2- to 50-fold molar excess, measured the free Cys-SH groups remaining, and then tested whether the Cys-SH groups could be regenerated by AhpF + NADH as assessed by the ability of the pretreated AhpC to carry out the reduction of TBH (a Cys-dependent process[12]) (Fig. 2a). AhpC regained over 90% of its TBH reductase activity following exposure to a 2-fold molar excess of peroxynitrite, even though the Cys-SH content fell from 1.7 to 0 mol Cys-SH per mol AhpC monomer. Each molecule of peroxynitrite led to the oxidation of 2 Cys (Fig. 2a inset). In contrast, nitration of AhpC became detectable only when peroxynitrite was at ≥10-fold molar excess over AhpC, and AhpC was not allowed to complete the catalytic cycle (Fig. 2a). Even at 50-fold molar excess of peroxynitrite over non-cycling AhpC, less than one of the five Tyr residues per AhpC monomer was detectably nitrated (Fig. 2b), a modification confirmed by immunoblot (Fig. 2c), and this was associated with irreversible crosslinking (Fig. 2b). Lower concentrations of peroxynitrite only caused disulphide bond formation (Fig. 2b). Thus, the first residues in AhpC to react with peroxynitrite are Cys, not Tyr, and the reaction leads to reversible disulphide bonding.

Spontaneous decomposition of peroxynitrite in pure solution leads to the accumulation of nitrate (~70%) and nitrite (~30%)[1]. In contrast, wild-type AhpC and C165A caused the nearly quantitative conversion of peroxynitrite into nitrite, while C46A and C46/165A were ineffective (Fig. 2d). Thus, AhpC catabolizes peroxynitrite to nitrite; Cys 46 is required, but Cys 165 and a reducing system are not.

Peroxynitrite might react with AhpC Cys 46 via either oxidation or nitrosation. We sought to trap a putative sulphenic acid intermediate through its reaction with 7-chloro-4-nitrobenz-2-oxa-1,3-diazole (NBD-Cl), which will react with Cys-SH or Cys-SOH, but not with Cys-SO_2H, Cys-SO_3H, Cys-SNO or Cys-SS-Cys[13]. To preclude formation of Cys-SS-Cys, we used C165A. We anaerobically reacted C165A sequentially with peroxynitrite and NBD-Cl and characterized the products by electrospray ionization mass spectrometry (Fig. 3). Untreated C165A yielded a single peak within 1 atomic mass unit (a.m.u.) of the predicted mass, 20,581 (Fig. 3a), and was modified by NBD (164 a.m.u.) to produce a peak at 20,745 a.m.u. (Fig. 3b). After pre-treatment with subequimolar peroxynitrite, the major peak shifted to 20,761 a.m.u., demonstrating that one atom of oxygen was incorporated (Fig. 3c). Decomposed peroxynitrite caused no peak shift, ruling out effects from any residual H_2O_2 in the preparation. When C46A was reacted with peroxynitrite and NBD-Cl, the major peak remained at 20,745 a.m.u. (Fig. 3d), indicating that Cys 46 is the site of oxidation.

Stopped-flow spectroscopy allowed us to quantify the reactivity of AhpC with peroxynitrite. Spontaneous decomposition of peroxynitrite at pH 7.0 and room temperature followed first-order kinetics with a rate constant of 0.51 ± 0.04 s^{-1}. Scans at 10-ms intervals over the first 100 ms were nearly superimposable (Fig. 4a). In contrast, in the presence of AhpC, peroxynitrite was completely decomposed within 100 ms (Fig. 4b) with a second-order rate constant of $1.51 \times 10^6\ M^{-1}\ s^{-1}$ (Table 1). The reaction was slowed by 2.5–3 orders of magnitude if the Cys residues in AhpC were first oxidized with TBH or mutated (Table 1). As a further control, β-lactamase, an enzyme of similar mass containing three Cys residues, purified from the same bacteria, reacted with peroxynitrite 1,600 times more slowly than AhpC (Table 1).

Cys residues that serve as catalytic sites often have low pKa values[14]. Consistent with this, the pH-dependence of the reactivity of C165A and C46A with a sulphydryl-alkylating agent revealed that the pKa for Cys 46 was < 5. In contrast, the pKa for Cys 165 was 8.7, close to that of free Cys. The pH optimum (6.72) for reaction of AhpC with peroxynitrite (Fig. 4d) is compatible with intracellular function.

Finally, AhpC homologues purified from two other phylogenetically distant pathogens, *M. tuberculosis* and *H. pylori*, reacted with peroxynitrite nearly as rapidly as AhpC from *S. typhimurium* (Fig. 4c; Table 1).

The remarkable rate of the reaction of peroxynitrite with AhpC, and the facility with which oxidized AhpC is reduced by AhpF or by the thioredoxin system, suggest that AhpC is likely to protect a cell from fluxes of peroxynitrite at sites where the intracellular concentration of AhpC is sufficiently high, and where the rate of peroxynitrite formation does not greatly exceed the reducing potential of a cell to replenish oxidized AhpC. The rates reported here for catabolism of peroxynitrite by bacterial peroxiredoxins are among the fastest known for peroxynitrite's reactions, despite the lack of haem and selenium. Cytochrome *c* oxidase, a haem protein, displayed peroxynitrite reductase activity ($10^6\ M^{-1}\ s^{-1}$)[15]. Under aerobic conditions, this reaction would be outcompeted by O_2 ($10^8\ M^{-1}\ s^{-1}$). Glutathione peroxidase, a selenoprotein, has the largest rate constant reported

Table 1 Second-order rate constants for peroxynitrite catabolism by bacterial peroxiredoxins and control proteins

Protein	Species	Pretreatment	Second-order rate constant ($M^{-1}\ s^{-1}$)
AhpC wild type	*S. typhimurium*	None	$1.51\ (\pm 0.04) \times 10^{6}$*
AhpC wild type	*S. typhimurium*	Oxidized	$3.00\ (\pm 0.06) \times 10^{3}$†
AhpC C165A	*S. typhimurium*	None	$5.52\ (\pm 0.19) \times 10^{4}$†
AhpC C46A	*S. typhimurium*	None	$6.30\ (\pm 0.05) \times 10^{3}$†
AhpC C46/165A	*S. typhimurium*	None	$2.44\ (\pm 0.04) \times 10^{3}$†
AhpC wild type	*M. tuberculosis*	None	$1.33\ (\pm 0.08) \times 10^{6}$*
AhpC wild type	*H. pylori*	None	$1.21\ (\pm 0.05) \times 10^{6}$*
β-lactamase	*E. coli*	None	$< 2.0 \times 10^{3}$‡

*Means ± s.d. of three experiments with independent preparations of protein each tested at multiple concentrations.
†Means ± s.d. of >3 runs at each protein concentration.
‡Mean from two experiments.

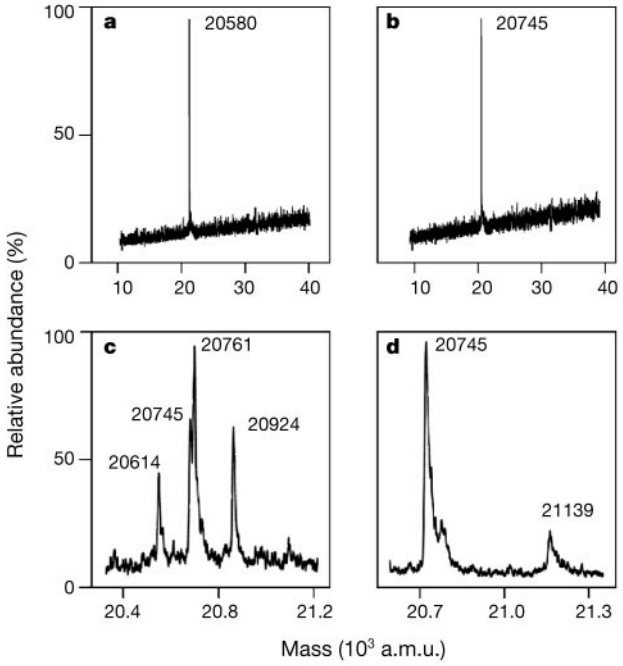

Figure 3 Sulphenic acid formation at Cys 46 in peroxynitrite-treated AhpC: identification by electrospray ionization mass spectrometry. **a**, AhpC C165A. **b**, NBD-modified AhpC C165A. **c**, NBD-modified AhpC C165A (100 μM) pretreated with peroxynitrite (75 μM). **d**, NBD-modified AhpC C46A pretreated with peroxynitrite as in **c**.

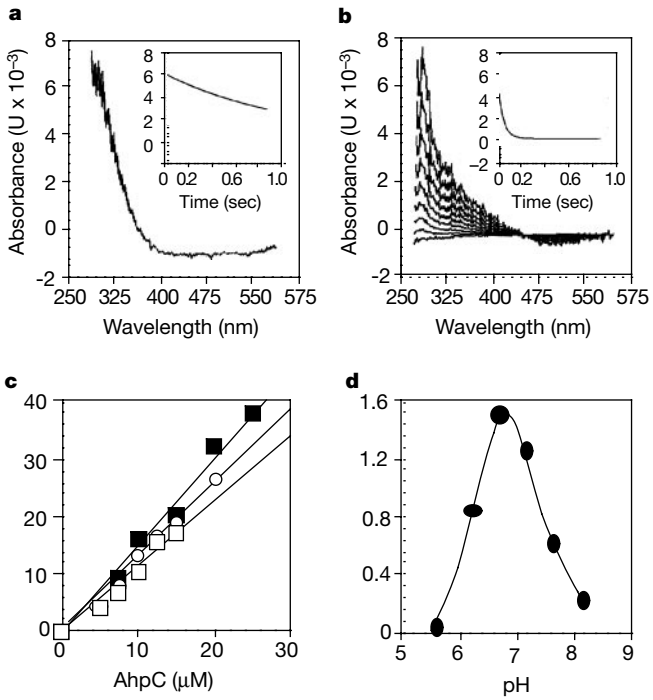

Figure 4 Kinetics of peroxynitrite catabolism by bacterial AhpC. **a**, Stopped-flow spectroscopy of peroxynitrite decomposition. Shown are nine overlying scans taken at 10-ms intervals after mixing. Inset, Time course monitored at 322 nm. **b**, Same as **a** except that AhpC (15 μM) was injected. **c**, Determination of second-order rate constants. Experiments were performed in the presence of increasing concentrations of AhpC purified from *S. typhimurium* (filled squares), *M. tuberculosis* (open circles) or *H. pylori* (open squares). Apparent second-order rate constants were determined from slopes of the plots shown. **d**, pH optimum. Values for k_{obs} were determined in KPi buffer with final pH ranging from 5.5 to 8.0 and corrected for spontaneous decomposition in the absence of AhpC at each pH.

for reaction of peroxynitrite with a physiological target (8×10^6 M^{-1} s^{-1})[16]. However, many species lack a glutathione system, including mycobacteria. Widespread expression[8] or overexpression[17] of AhpC by clinical isolates of *M. tuberculosis* may thus help explain their resistance to peroxynitrite[18].

The catalytic cycle of AhpC in reaction with alkylperoxide begins with formation of the cysteine sulphenic acid (Cys-OH) at Cys 46 (refs 13, 19). Disulphide bonding with Cys 165′ in the opposite chain of the AhpC dimer is followed by NADH-dependent reduction of the disulphide by AhpF (ref. 12). Our experiments show that the reaction between AhpC and peroxynitrite proceeds similarly, beginning with nucleophilic attack of the Cys 46 thiolate on the O–O bond, resulting in the transfer of one oxygen atom to Cys 46 and release of nitrite. There has been little previous evidence that reactive nitrogen intermediates can oxidize protein-bound Cys residues to Cys-SOH (ref. 20) or that oxidation of a biological molecule by reactive nitrogen intermediates can be reversible and functionally consequential. Nor is there precedent for a selenium-free Cys residue reacting as rapidly with peroxynitrite as does Cys 46 of AhpC. The special nature of this reaction is emphasized by the lack of a comparable reaction with free Cys (ref. 21), the Cys in glutathione, the three Cys in β-lactamase, the two free Cys involved in the catalytic cycle of AhpF, or Cys 165 of AhpC. Features of the microenvironment that may facilitate the reactivity of Cys 46 with peroxynitrite include its low pKa and the ability of intermonomeric disulphide bond formation to protect nascent Cys-OH from irreversible oxidation to the sulphinic or sulphonic acids.

In contrast to AhpC's ready reaction with peroxynitrite, we were unable to demonstrate any reaction of AhpC with NO, NO_2^- or *S*-nitrosoglutathione (data not shown). Nonetheless, *ahpC* protected cells against the bactericidal and cytocidal actions of NO_2^-, *S*-nitrosoglutathione and the products of NOS2 (ref. 8). This seeming contradiction can be resolved by hypothesizing that diverse forms of reactive nitrogen intermediates achieve or enhance their cytocidal potential after generating NO, which encounters O_2^-, resulting in conversion into peroxynitrite.

Most studies of the reaction of peroxynitrite with proteins have focused on tyrosine nitration[22], generally considered damaging and irreversible. However, a signalling role[23] is suggested by evidence that protein tyrosine nitration can be enzymatically reversed[24]. The demonstration that peroxynitrite can reversibly oxidize a protein active site Cys strengthens the possibility that low levels of peroxynitrite may participate in signal cascades. As precedent, some growth factors elicit production of H_2O_2, which temporarily inactivates tyrosine phosphatases through reversible formation of Cys-SOH at the active site, permitting protein tyrosine phosphorylation[25].

We have shown here that three peroxiredoxins from phylogenetically divergent pathogens all react extremely rapidly with peroxynitrite. Reactivity is based on reversible oxidation of the N-terminal Cys, a residue conserved throughout the superfamily. Thus, the ability to act as a peroxynitrite reductase may be shared by many peroxiredoxins. Reciprocally, the utility of the peroxynitrite reductase reaction may help account for the wide distribution of peroxiredoxins. Thus the present observations may have relevance for the control of host–pathogen interactions, inflammation, mutagenesis, ageing and homeostasis. □

Methods

Peroxynitrite was prepared by quenched-flow synthesis from acidified nitrite and hydrogen peroxide[26], and by biphasic synthesis from isoamyl nitrite and hydrogen peroxide[27] (product formation experiments; Fig. 2d).

Open reading frames (ORFs) of *ahpF*, *ahpC* and its mutants C46A, C165A and C46/165A from *S. typhimurium* were amplified by polymerase chain reaction (PCR) from pSty-CF (ref. 8). AhpC ORFs from *M. tuberculosis* and *H. pylori* were amplified by PCR from pPs-MtahpC (ref. 8) and ATCC NCTC 11637, respectively. ORFs were cloned into pET11c and expressed in *E. coli* BL21(DE3) (Novagen). AhpC from *S. typhimurium* and its mutants or AhpF were purified to homogeneity from isopropyl-1-thio-β-D-galactoside (IPTG)-treated cells by phenyl- (AhpC) or blue- (AhpF) sepharose and diethylaminoethyl (DEAE) chromatography[28]. AhpC homologues from *M. tuberculosis* and *H. pylori* were purified to homogeneity by phenyl sepharose and MonoQ (Pharmacia) anion exchange or gel filtration and MonoQ chromatography[29] respectively.

For the determination of pKa values, AhpC C46A and C165A (20 μM) were treated with iodoacetamide (200 μM) in 100 mM potassium phosphate, 1 mM EDTA at pH values from 4 to 10 for 45 min at room temperature. DTNB (5,5′-dithiobis(2-nitrobenzoic acid); 200 μM) was added, and sulphydryl content determined by absorbance at a wavelength of 412 nm.

Stopped-flow experiments were performed on an OLIS RSM-16 instrument. One syringe contained 5 μM peroxynitrite in 3 mM NaOH, and the other contained 100 mM potassium phosphate pH 7.0, 100 μM DTPA (KPi buffer). Equal volumes were injected into a stopped-flow cell, and the pH of the reaction (6.75) was measured at the outlet. 400 scans were collected for each run, and k_{obs} was obtained by fitting experimental data to a single exponential decay function.

TBH reductase activity was measured in the presence of NADH (200 μM), AhpF (500 nM) and AhpC (1 μM), and expressed relative to untreated AhpC. Sulphydryl content was measured with DTNB. Tyrosine nitration was measured by absorbance at 430 nm.

Received 6 June; accepted 10 July 2000.

1. Pfeiffer, S. *et al.* Metabolic fate of peroxynitrite in aqueous solution. Reaction with nitric oxide and pH-dependent decomposition to nitrite and oxygen in a 2:1 stoichiometry. *J. Biol. Chem.* **272,** 3465–3470 (1997).
2. Coddington, J. W., Hurst, J. K. & Lymar, S. V. Hydroxyl radical formation during peroxynitrous acid decomposition. *J. Am. Chem. Soc.* **121,** 2438–2443 (1999).
3. Merényi, G., Lind, J., Goldstein, S. & Czapski, G. Peroxynitrous acid homolyzes into ˙OH and ˙NO_2 radicals. *Chem. Res. Toxicol.* **11,** 712–713 (1998).
4. Niles, J. C., Burney, S., Singh, S. P., Wishnok, J. S. & Tannenbaum, S. R. Peroxynitrite reaction products of 3′,5′-di-O-acetyl-8-oxo-7,8-dihydro-2′-deoxyguanosine. *Proc. Natl Acad. Sci. USA* **96,** 11729–11734 (1999).
5. Wink, D. A. *et al.* Nitric oxide protects against cellular damage and cytotoxicity from reactive oxygen species. *Proc. Natl Acad. Sci. USA* **90,** 9813–9817 (1993).
6. Jin, D.-Y. & Jeang, K.-T. in *Antioxidation and Redox Regulation of Genes* (eds Sen, C. K., Sies, H. & Baeuerle, P. A.) 381–407 (Academic, New York, 2000).
7. Storz, G. *et al.* An alkyl hydroperoxide reductase induced by oxidative stress in *Salmonella typhimurium* and *Escherichia coli*: genetic characterization and cloning of *ahp*. *J. Bacteriol.* **171,** 2049–2055 (1989).
8. Chen, L., Xie, Q. & Nathan, C. Alkyl hydroperoxide reductase subunit C (AhpC) protects bacterial and human cells against reactive nitrogen intermediates. *Mol. Cell* **1,** 795–805 (1998).
9. Nathan, C. & Shiloh, M. U. Reactive oxygen and nitrogen intermediates in the relationship between mammalian hosts and microbial pathogens. *Proc. Natl Acad. Sci. USA* **97,** 8844–8848 (2000).
10. Wilson, T., de Lisle, G. W., Marcinkeviciene, J. A., Blanchard, J. S. & Collins, D. M. Antisense RNA to *ahpC*, an oxidative stress defence gene involved in isoniazid resistance, indicates that AhpC of *Mycobacterium bovis* has virulence properties. *Microbiology* **144,** 2687–2695 (1998).
11. Szabo, C., Zingarelli, B., O'Connor, M. & Salzman, A. L. DNA strand breakage, activation of poly (ADP-ribose) synthetase, and cellular energy depletion are involved in the cytotoxicity of macrophages and smooth muscle cells exposed to peroxynitrite. *Proc. Natl Acad. Sci. USA* **93,** 1753–1758 (1996).
12. Ellis, H. R. & Poole, L. B. Roles for the two cysteine residues of AhpC in catalysis of peroxide reduction by alkyl hydroperoxide reductase from *Salmonella typhimurium*. *Biochemistry* **36,** 13349–13356 (1997).
13. Ellis, H. R. & Poole, L. B. Novel application of 7-chloro-4-nitrobenzo-2-oxa-1,3-diazole to identify cysteine sulfenic acid in the AhpC component of alkyl hydroperoxide reductase. *Biochemistry* **36,** 15013–15018 (1997).
14. Claiborne, A. *et al.* Protein-sulfenic acids: diverse roles for an unlikely player in enzyme catalysis and redox regulation. *Biochemistry* **38,** 15407–15416 (1999).
15. Briviba, K., Kissner, R., Koppenol, W. H. & Sies, H. Kinetic study of the reaction of glutathione peroxidase with peroxynitrite. *Chem. Res. Toxicol.* **11,** 1398–1401 (1998).
16. Pearce, L. L., Pitt, B. R. & Peterson, J. The peroxynitrite reductase activity of cytochrome c oxidase involves a two-electron redox reaction at the heme a (3)-Cu(B) site. *J. Biol. Chem.* **274,** 35763–35767 (1999).
17. Sherman, D. R. *et al.* Compensatory *ahpC* gene expression in isoniazid-resistant *Mycobacterium tuberculosis*. *Science* **272,** 1641–1643 (1996).
18. Yu, K. *et al.* Toxicity of nitrogen oxides and related oxidants on mycobacteria: *M. tuberculosis* is resistant to peroxynitrite anion. *Tuber. Lung Dis.* **79,** 191–198 (1999).
19. Choi, H.-J., Kang, S. W., Yang, C.-H., Rhee, S. G. & Ryu, S.-E. Crystal structure of a novel human peroxidase enzyme at 2.0 A resolution. *Nature Struct. Biol.* **5,** 400–406 (1998).
20. Becker, K., Savvides, S. N., Keese, M., Schirmer, R. H. & Karplus, P. A. Enzyme inactivation through sulfhydryl oxidation by physiologic NO-carriers. *Nature Struct. Biol.* **5,** 267–271 (1998).
21. Radi, R., Beckman, J. S., Bush, K. M. & Freeman, B. A. Peroxynitrite oxidation of sulfhydryls. The cytotoxic potential of superoxide and nitric oxide. *J. Biol. Chem.* **266,** 4244–4250 (1991).
22. Beckman, J. S. & Koppenol, W. H. Nitric oxide, superoxide, and peroxynitrite: the good, the bad, and ugly. *Am. J. Physiol.* **271,** C1424–C1437 (1996).
23. Go, Y. M. *et al.* Evidence for peroxynitrite as a signaling molecule in flow-dependent activation of c-Jun NH(2)-terminal kinase. *Am. J. Physiol.* **277,** H1647–H1653 (1999).
24. Kamisaki, Y. *et al.* An activity in rat tissues that modifies nitrotyrosine-containing proteins. *Proc. Natl Acad. Sci. USA* **95,** 11584–11589 (1998).
25. Denu, J. M. & Tanner, K. G. Specific and reversible inactivation of protein tyrosine phosphatases by hydrogen peroxide: evidence for a sulfenic acid intermediate and implications for redox regulation. *Biochemistry* **37,** 5633–5642 (1998).
26. Koppenol, W. H., Kissner, R. & Beckman, J. S. Synthesis of peroxynitrite: to go with the flow or on solid grounds? *Methods Enzymol.* **269,** 296–302 (1996).
27. Uppu, R. M. & Pryor, W. A. Biphasic synthesis of high concentrations of peroxynitrite using water-insoluble alkyl nitrite and hydrogen peroxide. *Methods Enzymol.* **269,** 322–329 (1996).
28. Poole, L. B. & Ellis, H. R. Flavin-dependent alkyl hydroperoxide reductase from *Salmonella typhimurium*. 1. Purification and enzymatic activities of overexpressed AhpF and AhpC proteins. *Biochemistry* **35,** 56–64 (1996).
29. O'Toole, P. W., Logan, S. M., Kostrzynska, M., Wadstrom, T. & Trust, T. J. Isolation and biochemical and molecular analyses of a species-specific protein antigen from the gastric pathogen *Helicobacter pylori*. *J. Bacteriol.* **173,** 505–513 (1991).

Acknowledgements

We thank L. Chen for generating *ahpC* mutations, G. St John for the *H. pylori* clone, H. Erdjument-Bromage and P. Tempst for protein sequencing and T. Sakmar for access to his stopped-flow spectrophotometer. This work was supported by a Norman and Rosita Winston fellowship (R.B.) and by an NIH grant (C.N.).

Correspondence and requests for materials should be addressed to C.N. (e-mail: cnathan@med.cornell.edu).

Peptide cyclization catalysed by the thioesterase domain of tyrocidine synthetase

John W. Trauger*, Rahul M. Kohli*, Henning D. Mootz†, Mohamed A. Marahiel† & Christopher T. Walsh*

** Department of Biological Chemistry and Molecular Pharmacology, Harvard Medical School, 240 Longwood Avenue, Boston, Massachusetts 02115, USA*
† Biochemie/Fachbereich Chemie, Philipps-Universität Marburg, Hans-Meerwein-Strasse, 35032 Marburg, Germany

In the biosynthesis of many macrocyclic natural products by multidomain megasynthases, a carboxy-terminal thioesterase (TE) domain is involved in cyclization and product release[1,2]; however, it has not been determined whether TE domains can catalyse macrocyclization (and elongation in the case of symmetric cyclic peptides) independently of upstream domains. The inability to decouple the TE cyclization step from earlier chain assembly steps has precluded determination of TE substrate specificity, which is important for the engineered biosynthesis of new compounds[1]. Here we report that the excised TE domain from tyrocidine synthetase efficiently catalyses cyclization of a decapeptide-thioester to form the antibiotic tyrocidine A, and can catalyse pentapeptide-thioester dimerization followed by cyclization to form the antibiotic gramicidin S. By systematically varying the decapeptide-thioester substrate and comparing cyclization rates, we also show that only two residues (one near each end of the decapeptide) are critical for cyclization. This specificity profile indicates that the tyrocidine synthetase TE, and by analogy many other TE domains, will be able to cyclize and release a broad range of new substrates and products produced by engineered enzymatic assembly lines.

An enormous range of medicinally important polyketide and peptide natural products assembled by modular polyketide synthases (PKSs), non-ribosomal peptide synthetases (NRPSs) and mixed PKS/NRPS systems have macrocyclic structures, including the antibiotics erythromycin (PKS) and daptomycin (NRPS), the immunosuppressants cyclosporin (NRPS) and rapamycin (PKS/NRPS), and the antitumour agent epothilone (PKS/NRPS). PKSs and NRPSs are large, multifunctional proteins that are organized into sets of functional domains termed modules[1,2]. The order of modules corresponds directly to the sequence of monomers in the product. Synthetic intermediates are covalently tethered by thioester linkages to a carrier protein domain in each module. The thiol tether on each carrier domain is phosphopantetheine, which is attached to a conserved serine residue in the carrier protein in a post-translational priming reaction catalysed by a phosphopantetheinyltransferase[3]. Chain initiation involves loading a specific monomer onto the thiol tether of each carrier protein. Subsequent chain elongation steps involve transfer of the growing chain from an upstream carrier protein to the adjacent downstream carrier-protein-bound monomer. Release of the full-length chain